Supplementary materials for

Ferro- and ferrielectricity and negative piezoelectricity in thioamide-based supramolecular organic discotics

Indre Urbanaviciute[1], Miguel Garcia-Iglesias[2,3], Andrey Gorbunov[4], E. W. Meijer[2,5], Martijn Kemerink*[1,6]

[1] Complex Materials and Devices, Department of Physics, Chemistry and Biology (IFM), Linköping University, 58183 Linköping, Sweden.

[2] Institute for Complex Molecular Systems, Eindhoven University of Technology, Eindhoven P.O. Box 513, 5600 MB Eindhoven, the Netherlands;

[3] QUIPRE Department, Universidad de Cantabria, Avd. de Los Castros, 46, 39005 Santander, Spain.;

[4] Department of Applied Physics, Eindhoven University of Technology, PO Box 513, 5600 MB, Eindhoven, The Netherlands;

[5] Laboratory of Macromolecular and Organic Chemistry, Eindhoven University of Technology, Eindhoven P.O. Box 513, 5600 MB Eindhoven, the Netherlands;

[6] Institute for Molecular Systems Engineering and Advanced Materials, Heidelberg University, Im Neuenheimer Feld 225, 69120 Heidelberg, Germany.

* Corresponding author

E-mail: martijn.kemerink@cam.uni-heidelberg.de

Contents

1 Supplementary Methods

1.1 Synthetic procedures

ThioBTA-C8-S, **thioBTA-C12**, **BTA-C8-S** and **BTA-C12** were synthesized based on the procedures reported in Reference 1 and 2, respectively.

1.2 Device preparation, conditioning, and characterization

Thin film crossbar metal-ferroelectric-metal (MFM) capacitor devices for all probed **(thio)BTA** homologues were formed by spin-coating (700–2000 rpm) of a 30-40 mg/ml chloroform solution on chemically cleaned glass substrates with patterned aluminum bottom electrodes. Before thermal vacuum deposition of the aluminum top electrodes, the spin-coated films were annealed at 70°C for 15 min. to completely evaporate the solvent. The prepared MFM devices were 0.01–1 mm^2 in area, depending on the selected device. The typical film thickness was 300–700 nm, as measured by a Bruker Dektak XT profilometer.

In the as-cast organic ferroelectric films, the molecular columns lie in-plane to the electrode. When the molecular dipoles are oriented in this way, no polarization can be measured in the out-of-plane bottom-top electrode geometry. Therefore, prior to the electrical measurements, the devices are treated by a field annealing procedure when, at low viscosity conditions (≈60–100 °C) and with the help of an alternating external field, the molecular bundles are forced to stand perpendicularly to the electrodes. The procedure takes 10–180 seconds and accelerates with the applied field, its frequency and temperature. The subsequent cooling under applied field freezes the system in this quasi-orderly state; see Fig. S1 below.

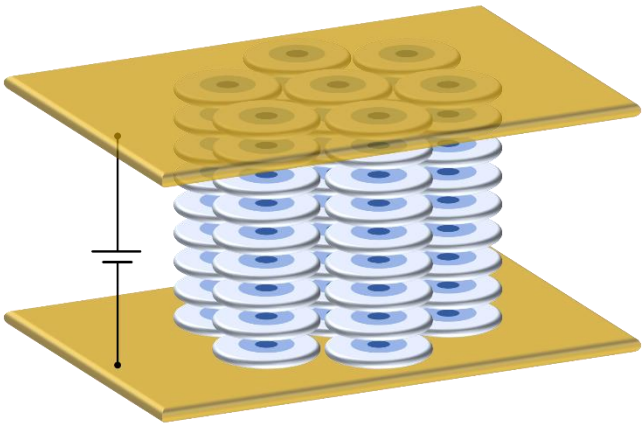

Figure S1. Schematic geometry of the measured out-of-plane devices after field annealing as described in the text. The applied field is parallel to the surface normal of the electrodes (dark yellow) and parallel to the axis of the supramolecular BTA stacks (blue).

The polarization loops are obtained by integration of the switching current transients. We use a quasi-static mode, better known as the Double Wave Method (DWM), when non-switching current is subtracted from the initial signal to avoid displacement and leakage inputs in the *P-E* curves.

Polarization retention measurements are performed using a similar DWM approach with a delay between the poling and probing signals. The devices are left at short circuit conditions during the waiting time. Each data point is measured after full repolarization. The device is considered depolarized when full polarization randomization is reached.

The input signal waveform is supplied by a Tektronix AFG3000 Arbitrary Function Generator and is amplified by a TREK PZD350A high voltage amplifier. The device response is visualized by a Tektronix TBS1000B Digital Oscilloscope.

The surface topography of spin-coated **(thio)BTA** films was studied by a Veeco Dimension 3100 atomic force microscope in tapping mode.

The thermal transitions were determined with Differential Scanning Calorimetry DSC using a Perkin–Elmer Pyris 1 DSC under a nitrogen atmosphere with heating and cooling rates of 10 $Kmin^{-1}$.

1.3 Piezoelectric characterization

Interferometry-based measurement techniques are a classical approach to characterize piezoelectric ceramics as well as thin-films by probing the converse piezoelectric response Being entirely contactless, the optical probe of the double-beam laser interferometer (DBLI) does not interact mechanically with the film, thus the response is measured with real electrodes in macroscopic, real-device conditions. The interferometric approach of the DBLI enables high precision measurements with angstrom accuracy. A vibration damping system is used to reduce the environmental noise. The equipment is of sufficient sensitivity and precision to measure the piezoelectric response in thin-films that typically give only small displacements, in the range of picometers. Compared to single-beam systems, the second reference laser beam (Mach–Zehnder interferometer) allows to compensate for possible substrate bending artefacts due to lateral piezoelectric activity. This is especially important for inorganic piezoelectric thin-films that are strongly clamped (usually, grown directly) on the substrate and have high piezoelectric constants. In case of organic piezoelectrics, this issue is less likely due to the very different physical properties of the film and the substrate and the rather weak mechanical coupling.

One important condition to get accurate results with the DBLI is the high reflectivity of both the top and bottom electrodes. In our case of glass/Al/**(thio)BTA**/Al devices, the thermally evaporated aluminum electrodes act as practically perfect mirrors. This is possible due to the typically very low surface roughness (of a few nanometers) of the **(thio)BTA** layers.

As mentioned above, due to the mechanical clamping of the piezoelectric layers on the substrate, the limited in-plane strain (corresponding to d_{31}) can effectively reduce the out-of-plane strain, as d_{31} and d_{33} are related by Poisson's ratio. The factually measured longitudinal piezoelectric coefficients are thus referred to as 'effective' and are typically lower than the real value for an unclamped film.

2 Further Experimental Results and Figures

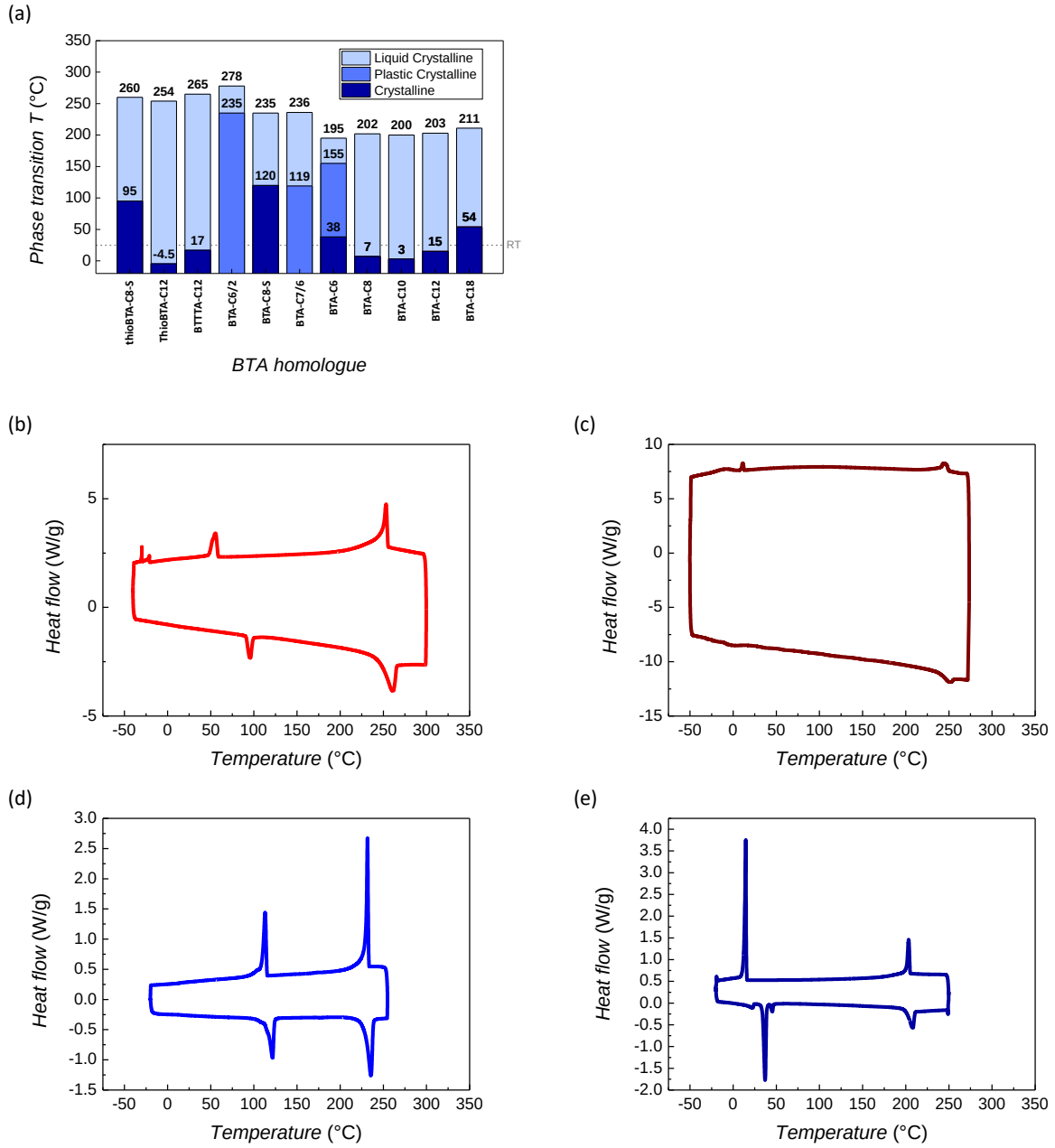

Figure S2. (a) Phase diagram of amide- and thioamide-based discotics with a demonstrated ferroelectric functionality. Data for BTA homologues C18, C12, C10, C8, C6, C7/6 and C6/2 is taken from Ref. [3,4] Data for BTT-cored trisamide BTTTA-C12 is taken from Ref. [5] (b-e) DSC thermograms for (b) thioBTA-C8-S, (c) thioBTA-C12, (d) BTA-C8-S, (e) BTA-C12.

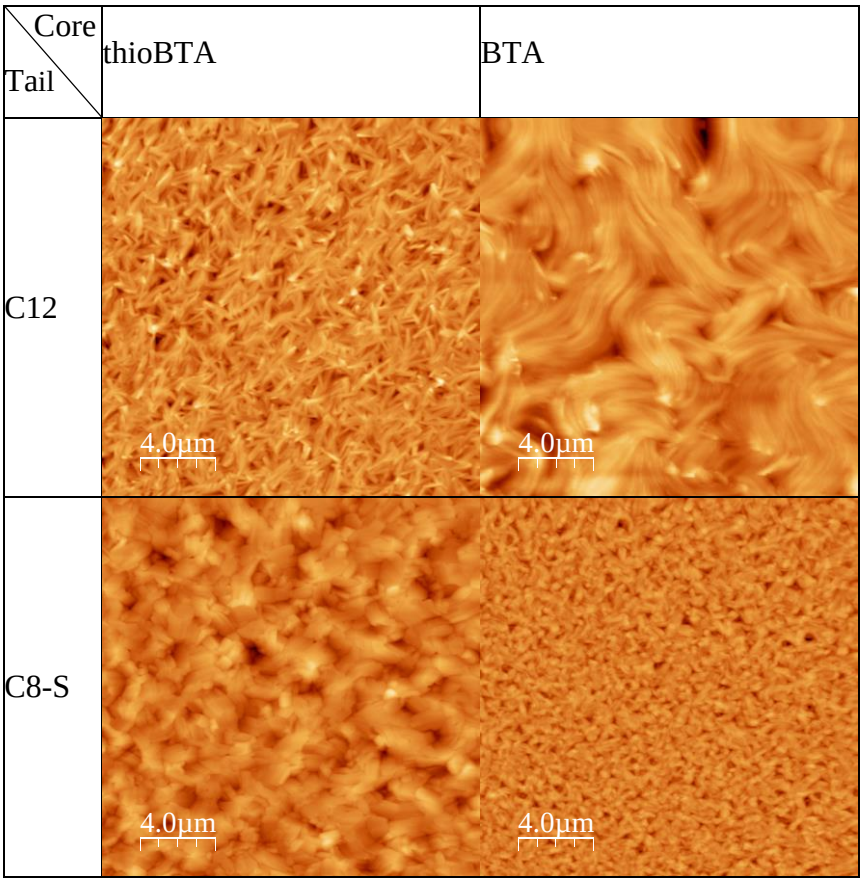

Figure S3. AFM micrographs obtained in tapping mode for (thio)BTA-C12 and (thio)BTA-C8-S at room temperature.

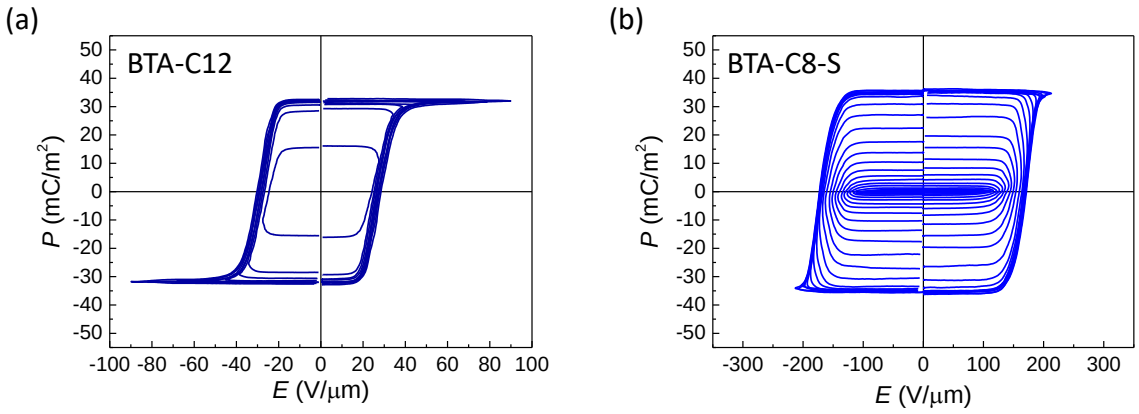

Figure S4. Saturating polarization hysteresis with inner loops of (a) BTA-C12 and (b) of BTA-C8-S obtained at 70°C, 25 Hz.

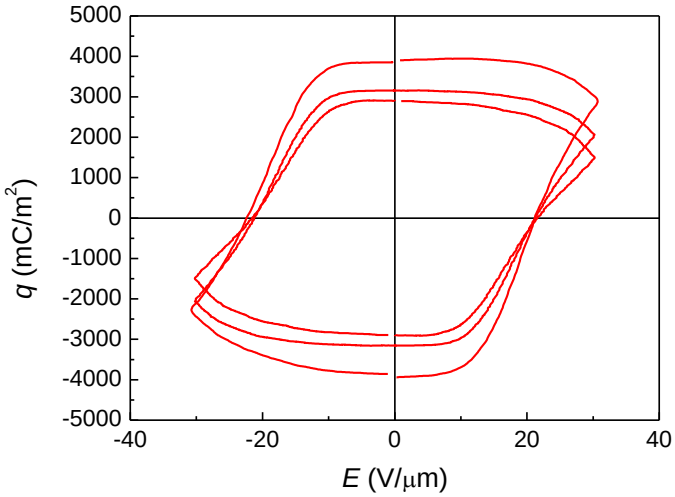

Figure S5. Extensive charge quantities are generated in thioBTA materials if noble metals (here Au) are used for the contacts. At elevated temperatures (here 100°C) and for slow voltage sweeping (here f = 0.005-0.02 Hz), an extensive amount of charge is found when integrating the polarization switching current transients. We tentatively attribute this effect to electrochemical reactions induced by sulfur in presence of noble metals. Note the absence of saturation with decreasing sweep speed in the otherwise reasonably normal looking hysteresis curves.

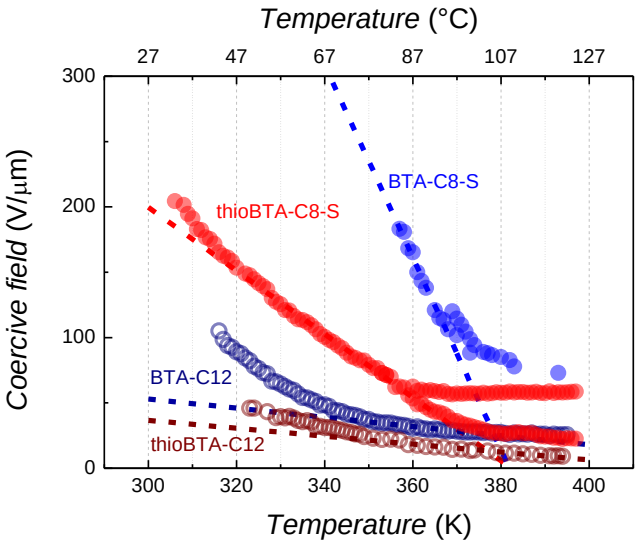

Figure S6. Coercive field versus temperature measurement results of the tested thioBTA and BTA materials at 25 Hz probing frequency. The deviation from a straight line at lower temperatures originates from an increase in voltage ramping speed of the probing signal. The extracted field-induced switching activation energy density based on Ref. [6] is significantly lower for the thioBTA-based homologues: thioBTA-C12 – 0.028 eV/nm^3, BTA-C12 – 0.035 eV/nm^3, thioBTA-C8-S – 0.26 eV/nm^3, BTA-C8-S – 0.53 eV/nm^3.

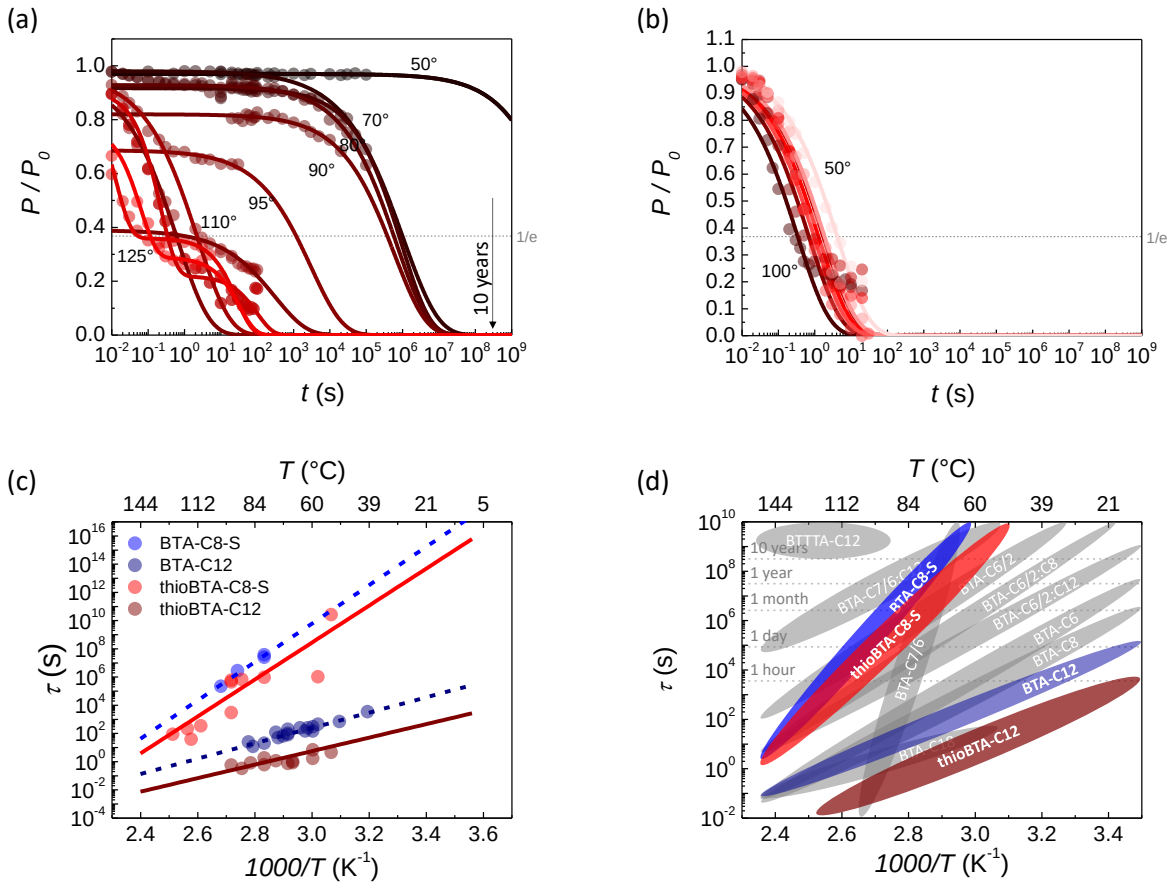

Figure S7. Depolarization kinetics of (a) thioBTA-C8-S and (b) thioBTA-C12 follow a stretched exponential trend, with the exception of thioBTA-C8-S at temperatures above 90-95°C where the material enters ferrielectric state. The extracted time constants are used to form an Arrhenius plot for depolarization activation (c) comparing thioBTAs (red shades, solid line) and BTAs (blue shades, dashed line), and (d) displaying the results in context of the previously reported trisamide-based ferroelectric materials from Ref.[3–5,7]. Lines in panel (c) indicate fits used for activation energy extraction, resulting in a depolarization barrier of 2.7 eV for BTA-C8-S, 2.6 eV for thioBTA-C8-S, 1.1 eV for BTA-C12, 0.95 eV for thioBTA-C12.

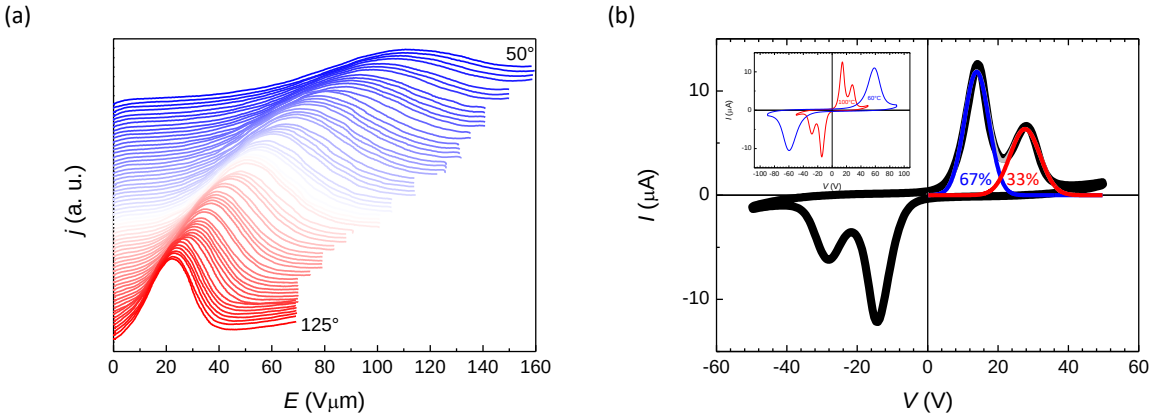

Figure S8. (a) ThioBTA-C12 temperature dependence of polarization switching current without any indications of double features, in contrast to thioBTA-C8-S. (b) Polarization switching current of thioBTA-C8-S at 100°C showing two distinct peaks with an integrated area ratio of 2:1 (67% and 33%). The inset demonstrates the distinction between switching current in ferroelectric (blue, 60°C) and ferrielectric (red, 100°C) state.

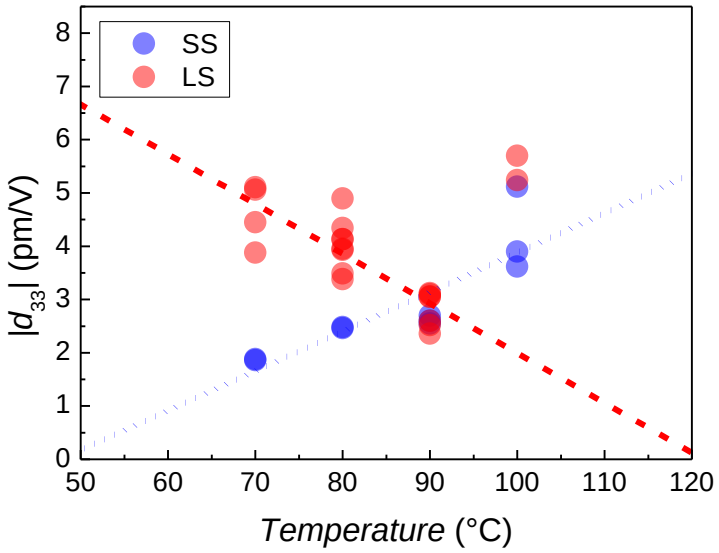

Figure S9. Temperature dependence of large-signal (red symbols) and small-signal (blue symbols) longitudinal piezoelectric constants of thioBTA-C8-S.

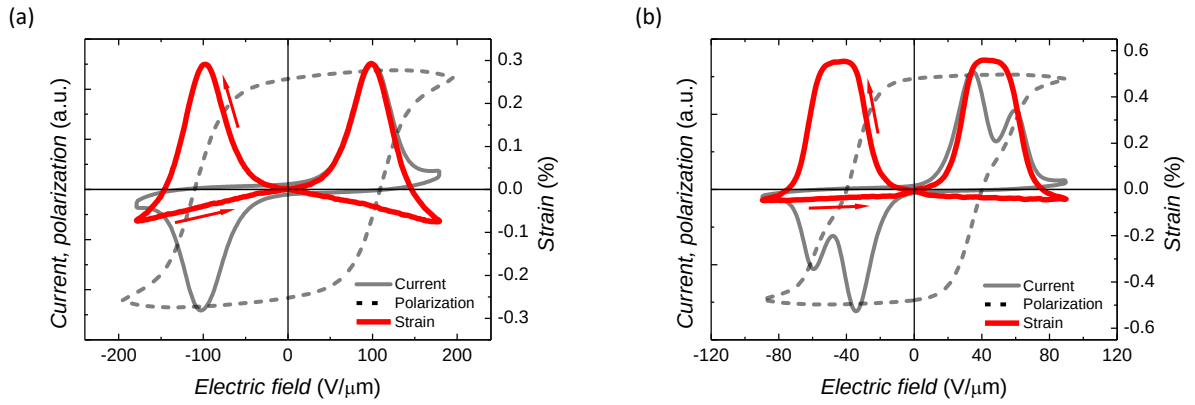

Figure S10. Switching current (black solid line), polarization (black dashed line), and large-signal strain (red line) loops of thioBTA-C8-S devices in a (a) ferroelectric state 80°C and (b) ferrielectric state 100°C.

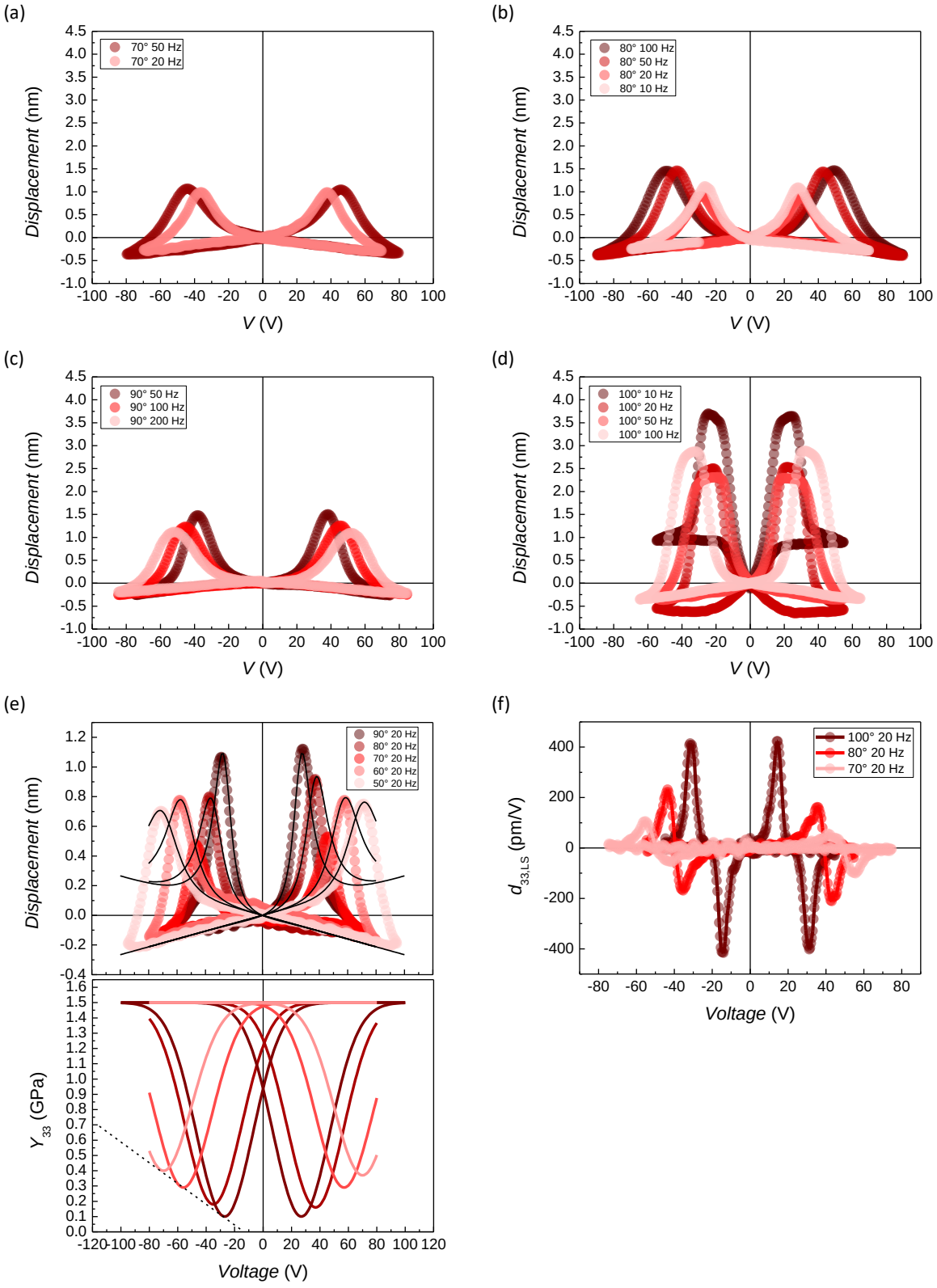

Figure S11. (a-d) Large-signal piezoelectric displacement butterfly loops measured at different temperature and probing frequencies, as indicated in legend. The anomalous form of the loops observed in panel (d) at 100°C 10-20 Hz can be explained by the effect of depolarization during the measurement procedure. (e) Fitting (black lines) of piezoelectric butterfly loops at different

temperature, taking into account the dynamic stiffness variation of Gaussian shape, as displayed in the bottom panel. The maximum stiffness value is approximate. (f) Dynamic piezoelectric constant acquired by differentiation of the large-signal displacement loops from panel (e), indicating extremely high transient values, exceeding 400 pm/V. Unlike for the long-tailed **BTA** homologues for which a significant Maxwell stress (negative quadratic strain-field dependence) was observed[8], no electromechanical response of non-piezoelectric nature was found for the **thioBTA-C8-S**, neither in the ferroelectric nor in the ferrielectric state.

3 Supplementary References

1. Mes, T. *et al.* Thioamides: Versatile Bonds To Induce Directional and Cooperative Hydrogen Bonding in Supramolecular Polymers. *Chem. - A Eur. J.* **19**, 8642–8649 (2013).
2. Stals, P. J. M. *et al.* Dynamic Supramolecular Polymers Based on Benzene-1,3,5-tricarboxamides: The Influence of Amide Connectivity on Aggregate Stability and Amplification of Chirality. *Chem. - A Eur. J.* **16**, 810–821 (2010).
3. Urbanaviciute, I. *et al.* Suppressing depolarization by tail substitution in an organic supramolecular ferroelectric. *Phys. Chem. Chem. Phys.* **21**, 2069–2079 (2019).
4. Urbanaviciute, I. *et al.* Tuning the Ferroelectric Properties of Trialkylbenzene-1,3,5-tricarboxamide (BTA). *Adv. Electron. Mater.* **3**, 1600530 (2017).
5. Casellas, N. M. *et al.* Resistive switching in an organic supramolecular semiconducting ferroelectric. *Chem. Commun.* **55**, 8828–8831 (2019).
6. Vopsaroiu, M., Blackburn, J., Cain, M. G. & Weaver, P. M. Thermally activated switching kinetics in second-order phase transition ferroelectrics. *Phys. Rev. B - Condens. Matter Mater. Phys.* **82**, 024109 (2010).
7. Urbanaviciute, I. *et al. Experimental indications for electrically switchable chirality in BTA*. (2022).
8. Urbanaviciute, I. *et al.* Negative piezoelectric effect in an organic supramolecular ferroelectric. *Mater. Horizons* **6**, 1688–1698 (2019).